Inflammopharmacology
https://doi.org/10.1007/s10787-025-01769-z

ORIGINAL ARTICLE

Bioactive potential of *Tripleurospermum inodorum* with detailed insight into anti-inflammatory activity through in vitro, in vivo evaluations and network pharmacology

Marija Ivanov[1] · Aleksandra Popov Aleksandrov[1] · Jelena Božunović[1] · Maria Inês Dias[2] · Ricardo C. Calhelha[2] · Jelena Kulaš[1] · Lillian Barros[2] · Isabel C. F. R. Ferreira[2] · Dejan Stojković[1]

Received: 17 December 2024 / Accepted: 26 March 2025

Abstract

This study evaluated *Tripleurospermum inodorum* extract for cytotoxic, anti-inflammatory, antioxidant, antimicrobial, and antibiofilm properties, alongside its phenolic profile, predicted pharmacological interactions and in vivo anti-inflammatory properties. The methanolic extract of *T. inodorum* was rich in apigenin derivatives, including apigenin-*O*-pentoside (5.234 mg/g) and apigenin-*O*-acetyl hexoside (4.929 mg/g), as identified using LC-DAD-ESI/MS^n. The extract demonstrated potent anti-inflammatory activity (IC_{50} = 8.4 µg/mL) by inhibiting nitric oxide production in a RAW 264.7 macrophage model, a key mechanism in controlling inflammatory responses. Its cytotoxicity against NCI-H460 lung carcinoma cells (GI_{50} = 62.9 µg/mL) suggests potential for targeting inflammation-driven carcinogenesis. Antioxidant activity, ranging from 204.4 (FRAP) to 442.2 (ABTS) mmol of gallic acid equivalents per 100 mg dry weight, highlights its role in mitigating oxidative stress—a critical driver of chronic inflammation. The extract also displayed moderate antimicrobial activity (MIC: 3–12 mg/mL) and strong antibiofilm potential (> 70% inhibition in a crystal violet assay), which are essential for managing infection-associated inflammation. Network pharmacology revealed that dominant phenolic compound act as aldose reductase inhibitors, targeting inflammatory pathways linked to metabolic stress. In vivo assessment using a xylene-induced ear edema model revealed a dose-dependent, biphasic anti-inflammatory effect, with lower doses (125 and 250 mg/kg) exhibiting greater efficacy compared to the highest dose (500 mg/kg), suggesting a hormetic response that emphasizes the importance of optimal dosing. These findings indicate that the methanolic extract of *T. inodorum* possesses a broad spectrum of bioactivities relevant to inflammation control and supports its further development as a source of novel anti-inflammatory therapeutics.

Keywords *Tripleurospermum inodorum* · Phenolics · Bioactivities · Inflammation · In vitro · In vivo

Introduction

The emerging need for novel therapeutics to address a range of illnesses and conditions such as infections (Ivanov et al. 2022) and inflammations (Attiq et al. 2018) underscores the urgency for innovative approaches in drug development. Advances in understanding disease mechanisms, coupled with technologies like network pharmacology, are pivotal in identifying new drug targets and therapeutic strategies. These efforts aim not only to enhance treatment efficacy but also to mitigate challenges such as drug resistance and side effects, thereby improving patient outcomes across various medical domains. Moreover, since ancient times, people have sought natural ways to cope with pathological conditions (Aware et al. 2022). Today, various modern approaches can be used to discover and develop plant-based therapeutics (Najmi et al. 2022). Additionally, it is now a well-established fact that both plants and their bioactive compounds exert numerous beneficial effects on human health, which are now scientifically proven (Nehru et al. 2024; Haridevamuthu et al. 2024). However, despite abundant research on plant-based bioactive matrices, much remains to be discovered

✉ Dejan Stojković
dejanbio@ibiss.bg.ac.rs

[1] Institute for Biological Research, Siniša Stanković", National Institute of the Republic of Serbia, University of Belgrade, Bulevar Despota Stefana 142, 11108 Belgrade, Serbia

[2] CIMO, LA SusTEC, Instituto Politécnico de Bragança, Campus de Santa Apolónia, 5300-253 Bragança, Portugal

Published online: 07 May 2025

regarding their full therapeutic potential and diverse pharmaceutical applications.

Network pharmacology studies are essential for elucidating the complex interactions between drugs and biological systems at a holistic level. By integrating data from multiple sources such as genomics, proteomics, and metabolomics, network pharmacology reveals the interconnected pathways and targets involved in disease mechanisms and drug action (Hopkins 2008). This approach facilitates the identification of novel drug targets, predicts adverse effects, and optimizes therapeutic efficacy (Li and Zhang 2013). Moreover, the network pharmacology enables the exploration of synergistic interactions among multiple compounds, providing new insights into polypharmacology and personalized medicine (Kibble et al. 2015).

Tripleurospermum inodorum (L.) Sch. Bip., commonly known as scentless mayweed, is a weed species that grows in various parts of Europe (Šuk et al. 2023). This plant belongs to Asteraceae family and is characterized by a phenotype resembling that of common chamomile (*Matricaria chamomilla*) (Šibul et al. 2019). Plants from the Asteraceae family are well known for their diverse bioactive properties, including anti-inflammatory, analgesic, antipyretic, along with their widely studied antioxidant potential (Bessada et al. 2015). Ethnobotanical data suggest that *Tripleurospermum* species have been used for a range of health applications, including their sedative, carminative, wound-healing, and anti-inflammatory properties, as well as for relieving muscle pain, fatigue, and sore throat. The phytochemical studies on *Tripleurospermum* species have revealed that they are rich in various bioactive compounds, including terpenes, hydrocarbons, steroids, oxygenated compounds, flavonoids, tannins, alcohols, acids, melatonin, and fragrant compounds (Lamponi et al. 2023).

The objective of our study was to comprehensively investigate the bioactive potential of *Tripleurospermum inodorum*, a commonly found weed whose medicinal properties remain largely unexplored. The study aimed to evaluate its cytotoxic, anti-inflammatory, antioxidant, antimicrobial, and antibiofilm activities. Furthermore, we analyzed the chemical composition of *T. inodorum*, with a particular focus on its phenolic constituents, and predicted their potential pharmacological targets. The rationale behind the broad concept of exploring anti-inflammatory, antioxidant, antimicrobial, and antibiofilm properties stems from the critical role of inflammation, oxidative stress, and infections—particularly those associated with biofilms—in the progression of various chronic diseases. These interconnected factors often drive the pathophysiology of many health conditions. By targeting these processes simultaneously, a more comprehensive and effective therapeutic approach can be developed. In light of the promising in vitro results showing significant anti-inflammatory activity, the study sought to deepen our understanding of *T. inodorum*'s anti-inflammatory potential, which emerged as the most pronounced biological feature observed in the plant's in vitro analysis. Accordingly, the xylene-induced ear edema model in Wistar rats was used to further examine the anti-inflammatory properties in vivo. This comprehensive strategy seeks to investigate the plant's wide range of bioactive compounds and how it might be used to treat different medical issues. By elucidating these aspects, the study sought to provide insights into the therapeutic potential of *T. inodorum* and contribute to the development of pioneering natural-based therapeutics for various health conditions.

Materials and methods

Collection of plant material and extraction procedure

Tripleurospermum inodorum (L.) Sch. Bip. (Asteraceae) was collected in Barelić, near Vranje, Serbia, in July 2022 during its flowering period and identified based on morphological characteristics by botanist Dr. Dejan Stojković. The dried plant samples were extracted with methanol, following the method previously described by Ćirić et al. (2019a, b).

Phenolic profile

Using LC-DAD-ESI/MSn (Dionex Ultimate 3000 UPLC, Thermo Scientific, San Jose, CA, USA), the extract's phenolic components were identified. After being separated, phenols were discovered (Bessada et al. 2016). A DAD (with favored wavelengths of 280, 330, and 370 nm) and a mass spectrometer (MS) performed a double online detection. A Linear Ion Trap LTQ XL mass spectrometer (Thermo Finnigan, San Jose, CA, USA) equipped with an ESI source performed the MS revelation in negative mode. Phenolics have been identified using information from the literature that provides a tentative identification, as well as data on their chromatographic performances and UV–Vis and mass spectra in comparison with the standard molecules, if available. The Xcalibur® data system (Thermo Finnigan, San Jose, CA, USA) has been used to acquire the data. The data from the UV–Vis signal were used to create a calibration curve for all relevant standards of phenolic compounds for quantitative analysis. In the event that the commercial standard chemical was unavailable, the detected molecules were quantified using the calibration curve of

the closest currently accessible standard. The quantitative findings were displayed as milligrams per gram of extract.

Cytotoxic potential: sulforhodamine B (SRB) assay

Human tumor cell lines AGS (gastric adenocarcinoma), $CaCo_2$ (colorectal adenocarcinoma), MCF-7 (breast adenocarcinoma), and NCI-H460 (lung carcinoma) were used in the assay. Vero cell line (African green monkey kidney) was used as a non-tumor cell line. Except for the Vero cell line, which was grown in DMEM medium + 10% FBS, glutamine, and antibiotics, all of the cell lines used in this test were grown in RPMI-1640 + 10% fetal bovine serum (FBS), 2 mM glutamine, 100 U/mL penicillin, and 100 mg/mL streptomycin. 37 °C and 5% CO_2 in a humidified environment were the conditions for cell incubation. When the cells reached 70% to 80% confluence, they were subjected to additional testing.

After dissolving 8 mg of the extracts in 1 mL of water to create stock solutions, the extracts were serially diluted to reach concentrations between 0.125 mg/mL and 8 mg/mL. The tested cell suspension (190 µL) and all individual extract concentrations (10 µL) were co-incubated for 72 h at 37 °C with 5% CO_2 in a humidified environment in microplates. Except for the Vero cell line, which was evaluated at 1.9×10^4 cells/well, other cell lines were analyzed at 10^4 cells/well.

Following incubation, the cell samples were prepared in the manner described below: the plates were incubated for 1 h at 4 °C with 100 µL of 10% (w/v) of previously cooled TCA before being water washed. After drying, samples were placed at room temperature for 30 min and supplemented with an SRB solution (0.057% m/v, 100 µL). The microplates were thoroughly cleaned with a 1% (v/v) acetic acid solution and then left to dry to remove any non-adhered SRB. Additionally, 200 µL of 10 mM Tris was used to dissolve the bound SRB, and the Biotek ELX800 microplate reader was used to measure the absorbance at 540 nm. The extract concentration that might 50% inhibit cell growth (GI50) was used to present the results. Ellipticine was used as a positive control in the tests.

Anti-inflammatory activity

H_2O was used to dissolve the extract (8 mg/mL). To get to the investigated doses (0.125–8 mg/mL), serial dilutions were carried out. The Leibniz-Institut DSMZ (Deutsche Sammlung von Mikroorganismen und Zellkulturen GmbH) RAW 264.7 mouse macrophage cell line was cultured in DMEM media supplemented with 10% heat-inactivated FBS, glutamine, and antibiotics. The cells were kept at 37 °C in a humid environment with 5% CO_2, and they were separated using a cell scraper.

Microplate wells were seeded with a 300-µL cell suspension, a density of 5×10^5 cells/mL, and a dead cell rate of less than 5% (as assessed by the Trypan blue exclusion test). To encourage cell adhesion and proliferation, the samples were cultured for 24 h under the aforementioned circumstances. Following this, the cells were treated for one hour with extract quantities that were serially diluted (15 µL, 0.125–8 mg/mL). 6.25–400 µg/mL was the final concentration range. 30 µL of a lipopolysaccharide (LPS) (1 µg/mL) was added to stimulate the cells, and this was followed by another 24-h incubation period. Representatives without LPS served as the negative control, and dexamethasone (50 µM) served as the positive control.

Using a nitrite calibration curve (100 µM sodium nitrite at 1.6 µM) and a Griess reagent system kit (including nitrophenamide, ethylenediamine, and nitrite solutions), nitric oxide was quantified in a 96-well microplate. An ELX800 Biotek microplate reader (Bio-Tek Instruments, Inc., Winooski, VT, USA) was used to measure absorbance at 540 nm and compare it with the standard calibration curve to estimate the production of nitric oxide. The concentration of T. inodorum extract that causes 50% inhibition of nitric oxide generation (IC50) was used to depict the results, which were calculated by graphically displaying the percentage inhibition of nitric oxide generation vs the concentration of samples.

Antioxidant activity

Ferric ion reducing antioxidant power: FRAP assay

To determine the ferric ion reducing antioxidant power (FRAP), several modifications were made to the procedure described by Benzie and Strain (Benzie and Strain 1996). The working FRAP reagents were 300 mM sodium acetate buffer (pH 3.6), 20 mM ferric chloride, and 10 mM ferric-2,4,6-tri(2-pyridyl)−1,3,5-triazine (Fe3 + -TPTZ) dissolved in 40 mM hydrochloric acid. The new working solution was made by mixing 3 mL of ferric chloride, 3 mL of FRAP reagent, and 30 mL of acetate buffer. 50 µL of the tested sample and 950 µL of freshly prepared FRAP reagent were combined to form each sample in triplicate, which was then allowed to sit at room temperature for 10 min. Absorbance at 593 nm was measured using an Agilent 8453 spectrophotometer (Agilent Technologies, Waldbronn, Germany). Gallic acid (GA) methanol solutions were used to create the calibration curve. The results are expressed in gallic acid equivalents (mmol GAE) per 100 mg of plant dry weight (DW). All analyses were performed three times.

DPPH radical scavenging activity

With some adjustments, the DPPH assay was carried out in accordance with previous instructions (Guru et al. 2021; Issac et al. 2021). 50 µL of the tested sample, 450 µL of methanol, and 500 µL of a 200 µM 1,1-diphenyl-2-picrylhydrazil (DPPH, Sigma Aldrich, Germany) solution made in methanol were combined to generate the reaction mixture. The absorbance was measured at 517 nm after an incubation time of 30 min at room temperature. The radical scavenging potential as a percentage of DPPH discoloration was calculated using the following formula:

$$\text{DPPH radical scavenging (\%)} = \left[(\text{Acontrol} - \text{Asample})/\text{Acontrol}\right] * 100,$$

with Asample being the solution absorbance with the extract/reference compound, and Acontrol is the sole DPPH solution absorbance.

The calibration curve was developed using GA methanol solutions and the results are shown as mmol GAE per 100 mg^{-1} plant DW. Three triplicates of the experiment were carried out.

ABTS radical cation scavenging activity

The modified procedure previously described served as the basis for the ABTS radical cation decolorization experiment (Re et al. 1999). To produce ABTS radical cations, equal amounts of 2.45 mM potassium persulfate and 7 mM ABTS (2,2'-azinobis(3-ethylbenzothiazoline-6-sulfonate)) were mixed and incubated for 12 h at room temperature in the dark. The solution was employed as the ABTS test reagent in the assay after being diluted with 80% ethanol after incubation (absorbance at 734 nm: 0.7 ± 0.02). Sample (30 µL) and ABTS test reagent (970 µL) were included in reaction mixtures, which were incubated for 10 min at room temperature. The absorbance at 734 nm was then measured.

ABTS% + radical scavenging activity (%) was determined by the following formula:

$$\left[(\text{Acontrol} - \text{Asample})/\text{Acontrol}\right] * 100,$$

where Asample is the solution absorbance with *T. inodorum* extract and Acontrol is the absorbance of the ABTS% + solution without extract added.

The calibration curve was developed using GA methanol solutions and the results are shown as mmol GAE per 100 mg^{-1} plant DW. Three triplicates of the experiment were carried out.

Antimicrobial activity

Candida isolates used in this study were clinical samples *C. albicans* 475/15, *C. albicans* 13/15, *C. albicans* 17/15, *C. krusei* H1/16, *C. glabrata* 4/6/15 and reference yeasts *C. albicans* ATCC 10231, *C. tropicalis* ATCC 750, *C. parapsilosis* ATCC 22019, and *C. auris* ATCC B 11903. Strains used in this assay were resistant strains—methicillin-resistant *Staphylococcus aureus* (IBRS MRSA 011), *Pseudomonas aeruginosa* (IBRS P001), *Escherichia coli* (IBRS E003) (Victor et al. 2018) and reference strains *Yersinia enterocolitica* (ATCC 23715), *Klebsiella pneumoniae* (ATCC 13883).

Microdilution assay was employed for the establishment of minimum inhibitory (MIC) and minimum fungicidal/bactericidal concentrations (MFC/MBC). Yeast or bacterial cultures (1.0×10^5 CFU/per well) were incubated in the 96-well microtiter plates with serially diluted *T. inodorum* in YPD broth (yeasts) and Tryptic Soy Broth (bacteria, TSB) at 37 ˚C, 24 h. Upon incubation, MIC and MFC/MBC values were obtained.

The lowest tested *T. inodorum* concentrations that were not promoting microscopically detectable growth under inverted microscope Nikon Eclipse TS2 (Amsterdam, Netherlands) and compared to the control (untreated yeast cells) were considered as MIC. MFC were presented as extract concentrations that do not induce visible yeast growth upon serial sub-cultivation of 10 µL of samples at 37 °C, 24 h. Ketoconazole (SigmaAldrich, Darmstadt, Germany) was employed in the assay as a commercial antifungal control drug.

The MIC values for bacteria were observed after the incubation of samples with iodonitrotetrazolium chloride (INT) (0.2 mg/mL, 40 mL) at 37 °C, 30 min. The lowest concentration that did not induce bacterial in comparison with the positive control was proposed as the MIC. The MBC was determined by serial sub-cultivation of 10 mL of each well sample into microplates containing 100 mL of the TSB. The lowest concentration that did not induce growth upon sub-culturing was determined as the MBC. Streptomycin (SigmaAldrich, Germany) was employed as positive control.

Antibiofilm activity

Potential of *T. inodorum* to impede with *C. albicans* 475/15 biofilm establishment was tested as previously explained (Ivanov et al. 2021). *Candida* was incubated with serially diluted extract (MIC, 0.5 MIC and 0.25 MIC) in YPD medium, by using 96-well plates with adhesive bottom (Sarstedt, Germany), at 37 °C during 24 h. Microtiter plate was washed twice with sterile PBS and methanol was added.

Upon cell fixation, methanol was aspirated and the microtiter plate was left to air dried. Crystal violet (0.1%, Bio-Merieux, France) was used for 30 min to stain the biofilms. The plate was tap water washed and air dried. Afterwards, the stain bound to biofilms was dissolved with ethanol (96%, Zorka, Serbia). Absorbance was determined on a Multiskan™ FC Microplate Photometer, Thermo Scientific™. The following equation was used to determine percentage of inhibition of biofilm formation:

$$\left[(\text{A620control} - \text{A620sample})/\text{A620control}\right] \times 100$$

Prediction of putative targets

The putative targets were identified by using the SwissTargetPrediction software (http://www.swisstargetprediction.ch/) while Cytoscape_v3.10.2 was used for the preparation of illustration network for compound-target interactions for the most abundant compounds detected in the *T. inodorum* sample.

Assessment of in vivo anti-inflammatory activity: xylene-induced ear edema in rats

We employed xylene-induced ear inflammation model (Fig. 1) to evaluate extract's in vivo anti-inflammatory effect (Sun et al. 2018). The experimental procedures and animal treatments complied with EEC Directive 2010/63/EU on the protection of animals used for experimental and other scientific purposes and were approved by the Ethical Committee of the Institute for Biological Research "Sinisa Stankovic" (IBISS), University of Belgrade, Serbia (ethical clearance number 01–126/25). Female Wistar rats (150–200 g) were housed under controlled conditions at IBISS (12 h light/dark cycle, 60% humidity, 21–24 °C). The animals were divided into five groups: Group 1 (control) received orally 1 mL of distilled H_2O, Groups 2, 3 and 4 received 1 mL of H_2O containing extract in doses 125, 250 and 500 mg/mL, respectively, and Group 5 received 1 mL of water containing 2 mg/mL dexamethasone (positive control). All rats received the designated treatment via oral gavage for four consecutive days. Ear edema was induced by applying 50 µL of xylene to the dorsal and ventral surfaces of the right ear, 30 min after the final oral treatment, while the left ear remained untreated. Ear thickness was measured using a digital caliper at 30 and 60 min following edema induction. Afterward, the animals were sacrificed, and ear samples were collected. A 10-mm round ear piece was taken from the same location on both the left (untreated) and right (xylene-treated) ears and weighed to assess differences in ear mass as an additional parameter of ear edema. The differences in thickness and mass between the right and left ears were used to determine the degree of ear edema.

Isolation of ear cells

Epidermal and dermal cells were isolated from right xylene-treated ear in all groups to analyze extract's effect on ear cells inflammatory response (Sumaria et al. 2011; Tucovic et al. 2022). The ears were separated into dorsal and ventral halves using forceps and digested with

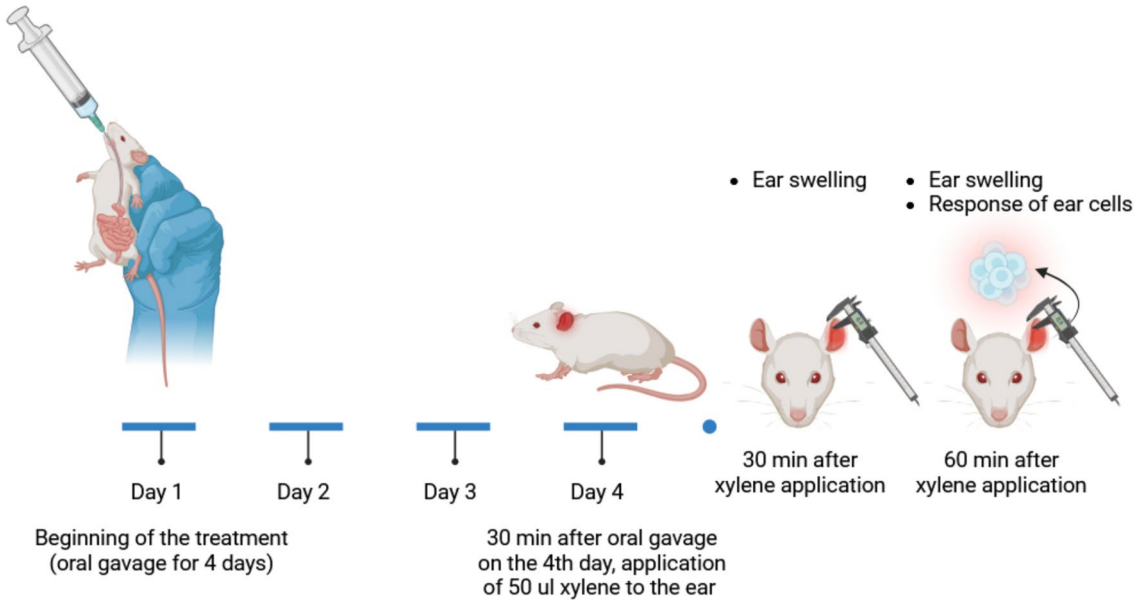

Fig. 1 Schematic representation of the in vivo xylene-induced ear edema model and treatment protocol

Dispase II (2.5 mg/mL) (Sigma-Aldrich, St. Louis, MO, USA) at 37 °C for 90 min to separate the epidermis and dermis. The separated layers were then cut into small pieces and further digested with collagenase type IV (1 mg/mL) and DNase I (1 mg/mL) at 37 °C for 45 min to release cells. The resulting tissue suspensions were filtered through a 70-µm nylon mesh (BD Bioscience, USA), washed, and resuspended in the medium to obtain single-cell suspensions. Ear cells (0.2×10^6/well) were cultured for 48 h at 37 °C, 5% CO_2 in 96-well plates. The cytokine levels were measured using commercially available ELISA kits for rat TNF and IL-6 (purchased from R&D, Minneapolis, USA), with titers calculated from a standard curve of recombinant cytokines. To assess cell metabolic viability, 100 µL of medium containing 10 µL of MTT salt (Sigma-Aldrich, St. Louis, MO, USA) was added immediately to freshly isolated cells and incubated for 3 h at 37 °C in a humidified atmosphere containing 5% CO_2. After incubation, 10% sodium dodecyl sulfate (SDS)–0.01 N HCl was added to dissolve the formed formazan, and the absorbance of extracted chromogen was measured at 540 nm using a spectrophotometer Biotek Synergy H1 Multimode reader (Winooski, VT, USA).

Statistical analysis

The experiments were performed in three repeats and results are presented as means ± standard errors. The data were statistically analyzed using the GraphPad Prism 9.0.0. The differences between experimental groups and control were compared by students t-test and one-way ANOVA. A p values ($^*p \leq 0.05$, $^{**}p \leq 0.01$, $^{***}p \leq 0.001$, $^{****}p \leq 0.0001$) were considered to be statistically significant.

Results and discussion

Chemical profiling of T. inodorum methanolic extract

In our study, the dominant polyphenolic compounds in *T. inodorum* methanolic extract were apigenin derivatives, specifically apigenin-*O*-pentoside (5.234 mg/g) and apigenin-*O*-acetyl hexoside (4.929 mg/g) (Table 1). A previous study on *T. inodorum* reported high levels of total phenolics and flavonoids (25.2–51.9 mg/g), as well as significant amounts of apigenin and its derivative apigenin-7-*O*-glucoside (Šibul et al. 2019). The extract was also rich in 5-*O*-caffeoylquinic acid (3.529 mg/g) (Table 1), which was also identified as one of the dominant polyphenolic compounds in the previous study (Šibul et al. 2019).

Table 1 Retention time (Rt), wavelengths of maximum absorption (λ_{max}), mass spectral data, tentative identification, and quantification (mg/g extract) of the phenolic compounds present in the methanolic extract of *T. inodorum*

Peak	Rt (min)	λmáx (nm)	$[M-H]^-$ (*m/z*)	MS^2 (m/z)	Tentative identification	*T. inodorum*
1	5.03	324	341	179(100),161(34)	Caffeic acid hexoside	0.571 ±0.017
2	5.66	308	337	191(10),163(100),119(13)	3-*O*-*p*-Coumaroylquinic acid	0.692 ±0.011
3	6.31	326	353	191(100),179(7),173(5),135(5)	5-*O*-Caffeoylquinic acid	3.529 ±0.127
4	7.31	326	353	191(100),179(5),173(9),135(3)	*trans* 5-*O*-Caffeoylquinic acid	1.155 ±0.079
5	8.64	347	593	473(30), 383(31), 353(66)	Apigenin-*C*-dihexoside	0.296 ±0.024
6	10.17	308	337	191(100),163(10),119(13)	5-*O*-*p*-Coumaroylquinic acid	0.876 ±0.03
7	12.46	314	431	269(100)	Apigenin-*O*-hexoside	0.96 ±0.047
8	16.2	367	463	301(100)	Quercetin-*O*-hexoside	1.006 ±0.04
9	17.83	346	447	285(100)	Luteolin-*O*-hexoside	1.523 ±0.049
10	19.12	326	447	285(100)	Kaempferol-*O*-hexoside	0.658 ±0.022
11	21.18	357	505	301(100)	Quercetin-*O*-acetylhexoside	0.961 ±0.001
12	21.75	337	431	269(100)	Apigenin-*O*-pentoside	5.234 ±0.268
13	22.42	341	489	285(100)	Luteolin-*O*-acetylhexoside	1.233 ±0.052
14	26.93	336	473	269(100)	Apigenin-*O*-acetylhexoside	4.929 ±0.039
					Total phenolic acids	6.824 ±0.17
					Total flavonoids	16.799 ±0.257
					Total phenolic compounds	47.245 ±0.855

Table 2 Cytotoxic and anti-inflammatory activity of the *T. inodorum* methanolic extract

	T. inodorum	Ellipticine	Dexamethasone
Cytotoxic activity GI_{50} (μg/mL)			
AGS	198.7 ± 19.3	1.23 ± 0.03	–
CaCo2	278.1 ± 27.2	1.21 ± 0.02	–
MCF-7	265.7 ± 25.5	1.02 ± 0.02	–
NCI-H460	62.9 ± 5.1	1.01 ± 0.01	–
VERO	272.8 ± 26.2	1.41 ± 0.06	–
Anti-inflammatory activity IC_{50} (μg/mL)			
RAW 246.7	8.4 ± 0.8	–	6.3 ± 0.4

GI_{50}—concentration of extract with the ability to inhibit cell growth by 50% and IC_{50}—concentration of each of the extracts that causes the 50% inhibition of nitric oxide production

Table 3 Antioxidant activity of *T. inodorum* methanolic extract

Test	mmol GAE per 100 mg DW
ABTS	442.2 ± 9.8
DPPH	277.8 ± 0.8
FRAP	204.4 ± 0.9

Cytotoxic and anti-inflammatory activity

The examined extract exhibited the highest toxicity towards NCI-H460 lung carcinoma (GI50 62.9 μg/mL). On the other hand, its toxicity to other tumor cell lines was similar to its GI50 towards normal cells (VERO) (Table 2). A previous study on the *T. inodorum* essential oil compound, matricaria ester, demonstrated cytotoxicity against *Artemia salina* (Suleimen et al. 2018). The cytotoxic potential of the extract may be attributed to the apigenin derivatives present, as a previous study found that other derivatives of apigenin, as well as apigenin itself, exhibited cytotoxicity (Smiljkovic et al. 2017).

Additionally, we established significant anti-inflammatory potential of *T. inodorum* extract (IC_{50} 8.4 μg/mL). The ethnobotanical indices highlight the anti-inflammatory potential of *Tripleurospermum* species (Lamponi et al. 2023). 5-Caffeoylquinic acid, which has been previously shown to reduce chemically induced inflammation in mice (Segheto et al. 2018), may contribute to the extract's anti-inflammatory potential. This dual activity of the extract, both cytotoxic and anti-inflammatory, suggests that it could be a valuable candidate for further investigation as a potential therapeutic agent.

Further contributing to the *T. inodorum* extract's overall pharmacological profile may be the diversity of multiple bioactive substances, such as flavonoids and phenolic acids. The extract is a fascinating topic for in-depth pharmacological and toxicological research because of the potential interactions between these chemicals that could increase its effectiveness.

Antioxidant activity

Antioxidant properties of the methanolic extract of *T. inodorum*, commonly known as scentless mayweed, were evaluated (Table 3). The antioxidant potential was measured using three assays: ABTS, DPPH, and FRAP, and the results are presented in mmol of gallic acid equivalents (GAE) per 100 mg of dry weight (DW). *T. inodorum* exhibited significant antioxidant activity across all three assays, with the highest potential determined in the ABTS assay, followed by DPPH, and then FRAP. This suggests that the extract has a strong ability to neutralize free radicals and reduce oxidative stress, which may have potential health benefits. The discrepancies in the values obtained from the three assays are expected due to the varying principles and sensitivity of each assay to different types of antioxidants present in the extract. Another *Tripleurospermum* plant, *T. insularum,* was also studied and exhibited promising antioxidant potential (Zeljković et al. 2015). Moreover, the methanol extract of *T. limosum* exhibited the highest DPPH, ABTS, and hydroxyl radical-scavenging potential among the different extracts tested in a previous study (Chen et al. 2022).

The observed antioxidant activity might be linked to the presence of various biologically active compounds identified in the extract. Phenolic acids such as caffeic acid hexoside and coumaroylquinic acids are well-known for their ability to scavenge free radicals. Flavonoids like apigenin-*C*-dihexoside, luteolin-*O*-hexoside, quercetin-*O*-hexoside and luteolin-*O*-hexoside could also contribute significantly to antioxidant activity (Crozier et al. 2010). Their ability to donate electrons contributes to the total antioxidant capacity of the extract.

The methanolic extract of *T. inodorum* exhibits strong antioxidant activity, which is consistent with its abundant phenolic acid and flavonoid makeup. These substances support the extract's historical use as an antioxidant-rich medicinal plant in addition to offering insights into its possible health advantages.

Anticandidal activity

The methanolic extract of *T. inodorum* has exhibited moderate anticandidal potential, with MIC values ≥ 3 mg/mL against different *Candida* strains. It has shown the most intense antifungal activity towards strains *C. albicans* 475/15, *C. albicans* 17/15, *C. albicans* ATCC 10231 and *C. parapsilosis* ATCC 22019 (MIC 3 mg/mL) while lowest

Table 4 The anticandidal activity of the *T. inodorum* methanolic extract in terms of MIC and MFC values (mg/mL)

Yeasts	*T. inodorum*		Ketoconazole	
	MIC	MFC	MIC	MFC
C. albicans 475/15	3	6	0.003	0.006
C. albicans 13/15	6	12	0.0016	0.05
C. albicans 17/15	3	6	0.0016	0.05
C. krusei H1/16	6	12	0.0016	0.003
C. glabrata 4/6/15	6	12	0.0016	0.006
C. albicans ATCC 10231	3	6	0.0016	0.006
C. tropicalis ATCC 750	6	12	0.0016	0.006
C. parapsilosis ATCC 22019	3	6	0.003	0.006
C. auris ATCC B 11903	12	> 12	–	–

antifungal potential was recorded towards *C. auris* ATCC B 11903 (Table 4). To the best of the authors' knowledge, the presented information is the first data on the anticandidal potential observed for *T. inodorum*.

Tripleurospermum auriculatum has been previously tested and exhibited antifungal potential against *Geotricum candidum*, *Candida albicans*, *C. tropicalis,* and *Aspergillus fumigatus*. The MIC of the *T. auriculatum* ethanol extract against the *C. albicans* strain tested was 0.98 µg/mL (Al-Saleem et al. 2018), which is lower than our result (3 mg/mL) for *T. inodorum*.

Antibacterial activity

Antibacterial potential of *T. inodorum* methanolic extract was moderate with MIC values ranging from 3 mg/mL (for *P. aeruginosa* IBRS P001, *Y. enterocolitica* ATCC 23715, and *K. pneumoniae* ATCC 13883) to 12 mg/mL (*S. aureus* IBRS MRSA 011) (Table 5).

Tripleurospermum disciforme extract has been previously tested and exhibited antimicrobial effects against *S. aureus* and *S. epidermidis* (MICs of 112 and 224 µg/mL, respectively) (Tofighi et al. 2015). In contrast, the MIC against methicillin-resistant *S. aureus* in our study was much higher (12 mg/mL).

Table 5 The antibacterial activity of the *T. inodorum* methanolic extract in terms of MIC and MBC values (mg/mL)

Bacteria	*T. inodorum*		Streptomycin	
	MIC	MBC	MIC	MBC
Staphylococcus aureus (IBRS MRSA 011)	12	> 12	0.1	–
Pseudomonas aeruginosa (IBRS P001)	3	6	0.05	0.1
Yersinia enterocolitica (ATCC 23715)	3	6	0.01	0.02
Klebsiella pneumoniae (ATCC 13883)	3	6	0.005	0.01
Escherichia coli (IBRS E003)	6	12	0.1	0.2

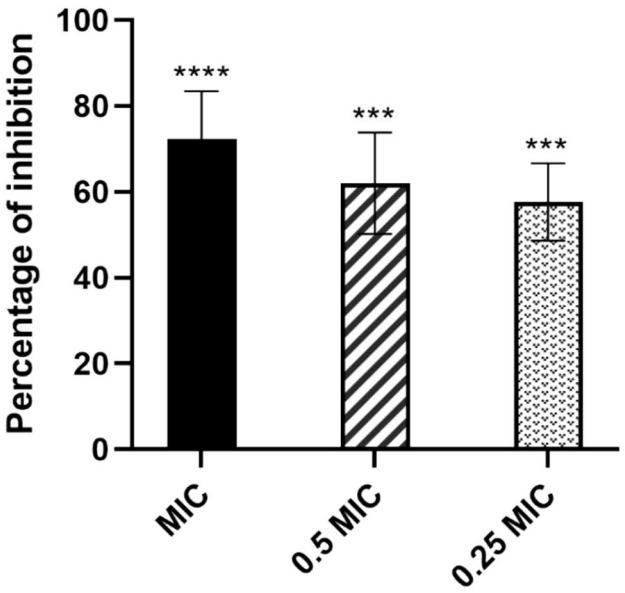

Fig. 2 Inhibition of *C. albicans* 475/15 biofilm formation upon treatment with the extract is presented as the mean value of three replicates ±SD. The asterisks represent statistical significance ***, $p \leq 0.001$, **** $p < 0.0001$ when treatment samples are compared with control (untreated sample, 0% inhibition)

Antibiofilm activity

The methanolic extract of *T. inodorum* exhibited promising antibiofilm potential when applied in concentrations ranging from 0.25 MIC to MIC. Formation of *C. albicans* 475/15 biofilm was significantly impaired especially when dose of MIC (3 mg/mL) was applied (Fig. 2). Previous antibiofilm investigation has been focused on the antibiofilm potential of diverse products such as silver nanoparticles (Muthulakshmi et al 2022) or piperine-coated zinc oxide nanoparticles (Shaik et al. 2024). Moreover, antibiofilm potential of plant extracts is well known (Ćirić et al. 2019a, b). However, according to the authors' best knowledge, this is the first study of *T. inodorum* antibiofilm potential.

Prediction of pharmacological targets

The network diagram was drawn to illustrate various molecular interactions and pathways potentially affected by plants dominant compounds (Fig. 3). The diagram centers around three compounds: apigenin-*O*-pentoside, apigenin-*O*-acetylhexoside and 5-*O*-caffeoylquinic acid, since they were the compounds with the highest detected quantities (Table 1). These compounds are connected to a number of targets, proteins, and enzymes, including interleukin-2, TNF-alpha, the

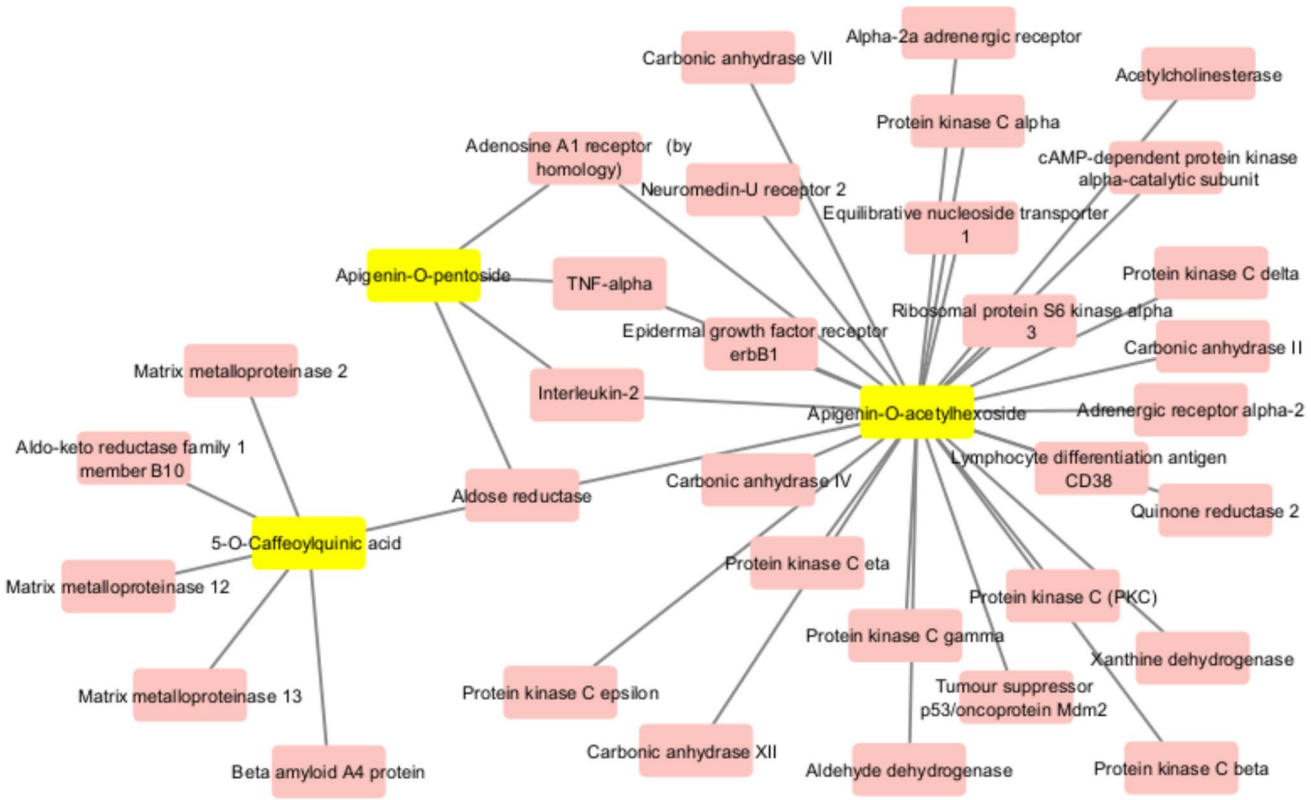

Fig. 3 Diagram representation of the most likely targets for the extract dominant compounds as detected by network pharmacology prediction

epidermal growth factor receptor (erbB1), and several more. Aldose reductase, matrix metalloproteinases, protein kinase C (alpha, beta, gamma, epsilon, delta), carbonic anhydrase (II, IV, VII, XII), and other proteins and enzymes are also part of the pharmacological network of these phytochemicals (2, 12, 13). Additionally displayed are certain receptors such as the adrenergic receptor alpha-2, neuromedin-U receptor 2, and adenosine A1 receptor.

Aldose reductase is the enzyme that is directly inhibited by all three compounds: apigenin-*O*-pentoside, apigenin-*O*-acetyl hexoside, and 5-*O*-caffeoylquinic acid. This implies that these compounds may work in tandem to block aldose reductase, which could result in a stronger reduction of glucose to sorbitol. Since aldose reductase is a crucial component of the polyol pathway, which is linked to the development of diabetic neuropathy, retinopathy, and nephropathy, this could have a big impact on how diabetic problems are treated (Dănilă et al. 2024). Although the polyol pathway is mainly linked to issues from diabetes, some research indicates that it may also have a role in the development of cancer. By interfering with the polyol pathway, inhibiting aldose reductase may have anti-cancer properties (Tammali et al. 2011). The polyol pathway contributes to ROS generation by depleting NADPH and GSH and enhancing NADH oxidation during the conversion of sorbitol to fructose. As the key rate-limiting enzyme in this pathway, aldose reductase (AR) drives the expression of inflammatory cytokines, including TNF-α and NF-κB.

Apigenin-*O*-pentoside and apigenin-*O*-acetylhexoside directly inhibit TNF-alpha and also have a connection to interleukin-2. This suggests that the compounds might have a role in regulating the immune response by influencing both pro-inflammatory (TNF-alpha) and anti-inflammatory (interleukin-2) cytokines. While inflammation is a complex process, some studies suggest that chronic inflammation can contribute to cancer development. Therefore, inhibiting TNF-alpha could potentially have anti-cancer effects by reducing inflammation (Zia et al. 2020). Both compounds have a connection to adenosine 1 receptor. Adenosine 1 receptor is involved in different physiological processes, such as inflammation, pain, and neurotransmission (Haddad et al. 2023). This connection suggests that the two compounds might have a role in modulating these processes through its interaction with adenosine 1 receptor.

Apigenin-*O*-acetylhexoside may also inhibit protein kinase C (PKC) alpha, according to connections. Inhibiting PKC alpha, a crucial enzyme involved in a number of signal transduction cascades, may have consequences for a number of illnesses, such as diabetes, cancer, and neurological disorders. It is possible that apigenin-*O*-acetylhexoside

inhibits PKC delta. PKC delta is involved in a number of cellular functions, including apoptosis, and diseases including cancer and neurological problems may be affected if it is inhibited (Lien et al. 2021).

As demonstrated in the in vitro tests, the extract's anticancer (cytotoxic) properties may be related to a possible interaction between the most prevalent phytochemicals and enzymes implicated in the development of cancer. Additionally, we demonstrated anti-inflammatory properties in vitro using a macrophage cell line model system, which may also potentially be connected to the enzyme inhibition mentioned above.

Extract anti-inflammatory activity in xylene-induced ear edema model in rats

Ear swelling, assessed by both thickness (Fig. 4) and weight (Fig. 5), was significantly reduced upon treatment with *T. inodorum* (Fig. 6). The extract at doses 125 mg/kg and 250 mg/kg significantly reduced xylene-induced ear edema, measured by both ear thickness and mass, similarly as dexamethasone (2 mg/kg), compared xylene-induced ear edema in H_2O-treated control group. However, this effect was absent at 500 mg/kg extract dose. In the model of xylene-induced ear edema, the study found that *T. inodorum* methanolic extract had a biphasic (hormetic) impact, indicating that lower dosages (125 and 250 mg/kg) were more successful in lowering inflammation than the highest dose (500 mg/kg). According to this response pattern, *T. inodorum* works through a dose-dependent but non-linear mechanism to reduce inflammation. Moderate dosages are the more effective, whereas the highest dose used caused a loss of efficacy or even a minor pro-inflammatory response. This biphasic pattern, which is frequently observed during hormesis, may be brought on by metabolic feedback loops, paradoxical stress reactions at elevated doses, or differential receptor activation (Calabrese 2014).

A similar pattern was seen in the NO production (Fig. 7), where intermediate doses (125 and 250 mg/kg) considerably decreased NO levels, however the 500 mg/kg dose had a

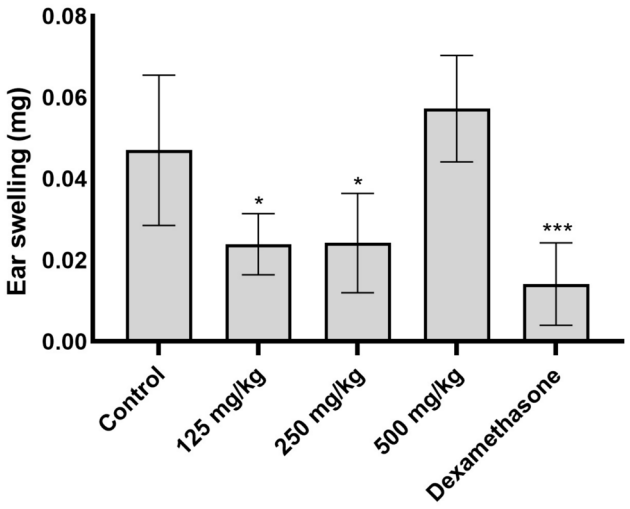

Fig. 5 Ear swelling (mg) upon treatment with *T. inodorum* (125, 250 and 500 mg/kg) and dexamethasone (2 mg/kg). Results are presented as mean values of three replicates ± SD. The asterisks represent statistical significance (*p ≤ 0.05, ***, p ≤ 0.001) when treatment samples are compared with control (sample treated with water)

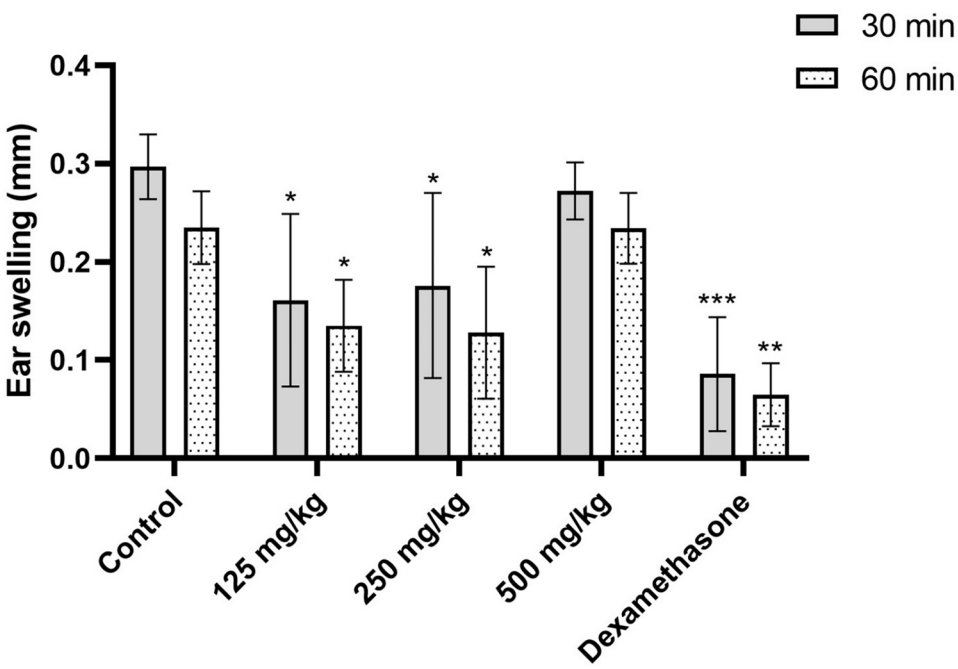

Fig. 4 Ear swelling (mm) upon 30 min and 60 min exposure to *T. inodorum* (125, 250 and 500 mg/kg) and dexamethasone (2 mg/kg). Results are presented as mean values of three replicates ± SD. The asterisks represent statistical significance (*p ≤ 0.05, ** ≤ 0.01, ***, p ≤ 0.001) when treatment samples are compared with control (sample treated with water)

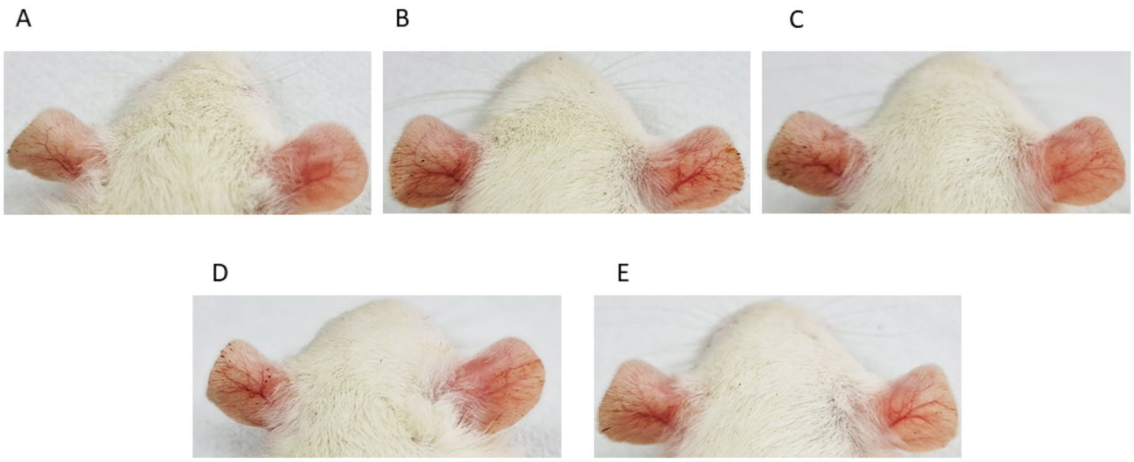

Fig. 6 Xylene-induced thickness of the right ear in A) control B) treatment with *T. inodorum* (125 mg/kg), C) treatment with *T. inodorum* (250 mg/kg), D) treatment with *T. inodorum* (500 mg/kg), E) dexamethasone (2 mg/kg)

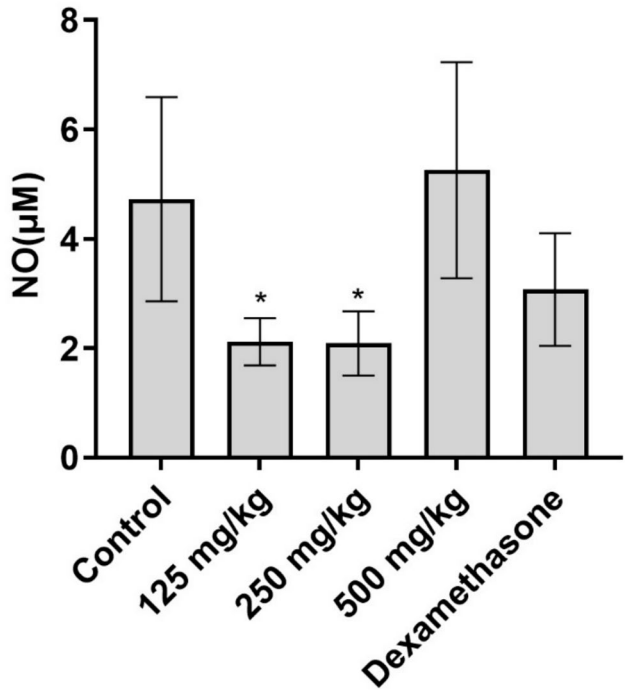

Fig. 7 Production of NO (μM) upon treatment with *T. inodorum* (125, 250 and 500 mg/kg) and dexamethasone (2 mg/kg). Results are presented as mean values of three replicates ± SD. The asterisks represent statistical significance (*p ≤ 0.05) when treatment samples are compared with control (sample treated with water)

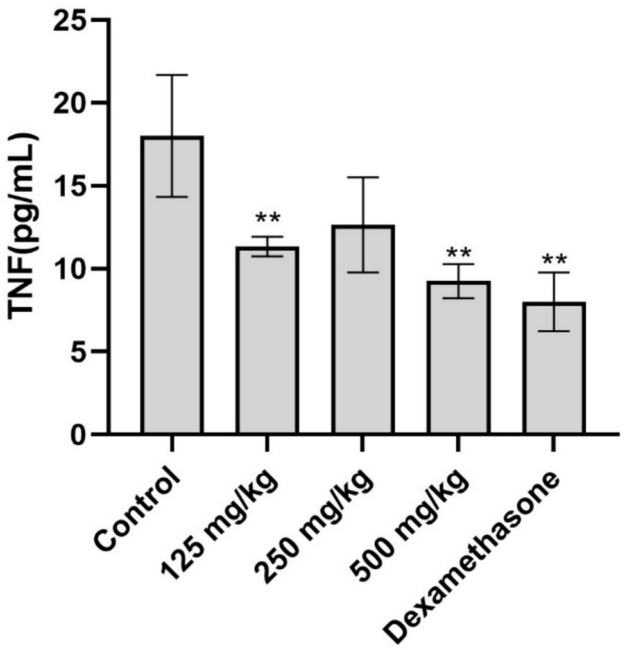

Fig. 8 Production of TNF (pg/mL) upon treatment with *T. inodorum* (125, 250 and 500 mg/kg) and dexamethasone (2 mg/kg). Results are presented as mean values of three replicates ± SD. The asterisks represent statistical significance (** ≤ 0.01) when treatment samples are compared with control (sample treated with water)

non-favorable impact. The decrease at lower dosages implies a strong anti-inflammatory effect, since NO is essential for vasodilation, oxidative stress, and immune cell activation (Andrabi et al. 2023). Higher concentrations, however, may cause cells to activate compensatory mechanisms in an attempt to counteract excessive NO suppression, making the response less efficient. The reduction in ear edema was accompanied by decrease in proinflammatory response of ear cells, indicated by lower production of NO, TNF (Fig. 8) and IL-6 (Fig. 9), in animals treated with extract at doses 125 mg/kg and 250 mg/kg (although TNF reduction at 250 mg/kg showed numerical decrease, p = 0,08), as well as dexamethasone. In animals that received 500 mg/kg of the

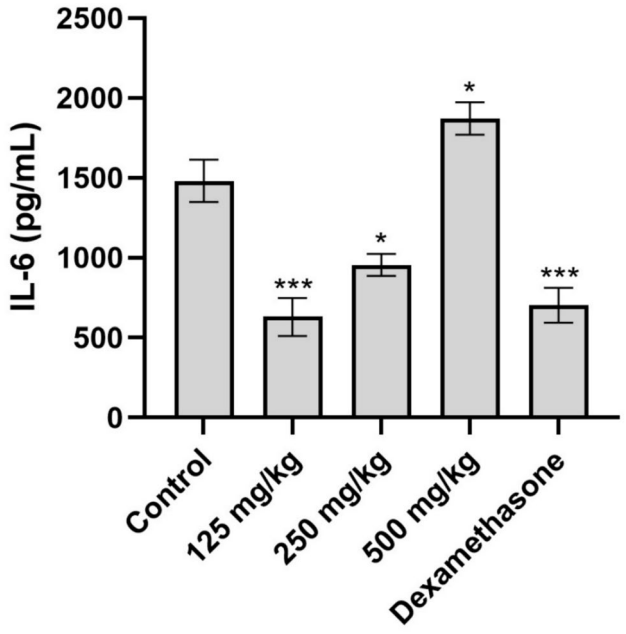

Fig. 9 Production of IL-6 (pg/mL) upon treatment with *T. inodorum* (125, 250 and 500 mg/kg) and dexamethasone (2 mg/kg). Results are presented as mean values of three replicates ± SD. The asterisks represent statistical significance (*p ≤ 0.05, ** ≤ 0.01, ***, p≤ 0.001) when treatment samples are compared with control (sample treated with water)

extract, NO production by ear cells remained unchanged, TNF decreased while IL-6 production was significantly increased, compared to controls.

No differences in ear cells metabolic viability were observed between groups (0,224 ± 0,108, 0,269 ± 0,086, 0,302 ± 0,019, 0,216 ± 0,018 and 0,236 ± 0,028 for controls, 125 mg/kg, 250 mg/kg, 500 mg/kg and dexamethasone, respectively).

The hormetic dose–response paradigm, which states that larger doses produce compensatory or paradoxical effects while low-to-moderate doses induce advantageous adaptive responses (Agathokleous and Calabrese 2019), is consistent with the observed biphasic pattern in *T. inodorum*'s anti-inflammatory efficacy. Among the explanations that could be offered are: (a) differential receptor activation; (b) balance of antioxidants and prooxidants; (c) metabolic adaptation and (d) hormesis and immune priming. Certain phytochemicals may function as partial agonists or modulators, causing compensatory effects at greater doses while activating anti-inflammatory pathways at lower concentrations. At low concentrations, polyphenols and flavonoids frequently show antioxidant benefits; but, at greater concentrations, they can cause mild oxidative stress, which may stimulate immune cells instead of suppressing them (Nitti et al. 2022). The extract's potency may be diminished by immune and inflammatory cells that downregulate receptor sensitivity or activate counter-regulatory pathways at high concentrations. While higher dosages of phytochemicals may encourage tolerance or compensatory activation, low-to-moderate doses may elicit a protective response, priming the immune system for upcoming challenges.

Conclusion

The methanolic extract of *T. inodorum* demonstrates significant bioactivity, primarily attributed to its rich polyphenolic composition. Its most notable effect is its strong anti-inflammatory activity, supported by substantial antioxidant and antibiofilm properties. The extract also exhibited promising cytotoxic potential against certain cell lines, likely due to the synergistic effects of its dominant phytochemicals. While its antimicrobial activity was moderate, it required relatively high concentrations to be effective. Significant inhibition in biofilm formation was noted upon addition of sub-inhibitory concentrations of the extract. Overall, *T. inodorum* showcases a diverse bioactivity spectrum relevant to inflammation control and warrants further investigation to explore its potential applications in anti-inflammatory therapeutics and other bioactive formulations. The results from in vivo tests demonstrate that *T. inodorum* has a complicated, dosage-dependent effect, with the strongest anti-inflammatory efficacy occurring at lower doses (125–250 mg/kg) compared to the maximum dose (500 mg/kg). A critical factor for prospective clinical applications is that this biphasic response implies that maximum efficacy is attained within a particular concentration range and that greater doses do not always improve therapeutic effects. In addition to its anti-inflammatory activity, the study also explored wide spectrum of extract's bioactivities such as antioxidant, antimicrobial, and antibiofilm properties, enhancing our knowledge on potential utilization and therapeutic development based on this plant. These findings shed light on the *T. inodorum* potential as the plant with diverse functions and potentially diverse applications in therapeutic formulations.

Author contributions Conceptualization, M.I. and D.S.; methodology, M.I., D.S., J.B., R.C. and M.I.D.; antimicrobial, antioxidant, cytotoxic, anti-inflammatory, and antibiofilm analysis, M.I. J.B., R.C. and D.S.; in vivo assays, A.P.A. and J.K.; phenolic content M.I.D and L.B..; data curation, M.I., M.I.D. and I.C.F.R.F.; writing—original draft preparation, M.I.; writing—review and editing, D.S.; supervision, L.B., I.C.F.R.F. and D.S.; project administration, L.B. and D.S.

Funding This research was funded by Ministry of Science, Technological Development and Innovation of the Republic of Serbia, Grant No 451-03-136/2025-03/200007. FCT/MCTES (PIDDAC): CIMO, UIDB/00690/2020 (DOI: 10.54499/UIDB/00690/2020) and UIDP/00690/2020 (DOI: 10.54499/UIDP/00690/2020); and SusTEC, LA/P/0007/2020 (DOI: 10.54499/LA/P/0007/2020); and national

funding by FCT, P.I., through the institutional scientific employment program contract for L. Barros, M.I. Dias, and R. Calhelha contracts.

Availability of data and materials Data will be made available on request.

Declarations

Conflict of interest The authors declare that there are no conflicts of interest.

References

Agathokleous E, Calabrese EJ (2019) Hormesis: *the dose response for* the 21st century: the future has arrived. Toxicol 425:152249. https://doi.org/10.1016/j.tox.2019.152249

Al-Saleem MS, Awaad AS, Alothman MR, Alqasoumi SI (2018) Phytochemical standardization and biological activities of certain desert plants growing in Saudi Arabia. Saudi Pharm J 26:198–204. https://doi.org/10.1016/J.JSPS.2017.12.011

Andrabi SM, Sharma NS, Karan A, Shahriar SMS, Cordon B, Ma B, Xie J (2023) Nitric oxide: physiological functions, delivery, and biomedical applications. Adv Sci (Weinh) 10:e2303259. https://doi.org/10.1002/advs.202303259

Attiq A, Jalil J, Husain K, Ahmad W (2018) Raging the war against inflammation with natural products. Front Pharmacol 9:412989. https://doi.org/10.3389/FPHAR.2018.00976/BIBTEX

Aware CB, Patil DN, Suryawanshi SS et al (2022) Natural bioactive products as promising therapeutics: A review of natural product-based drug development. S Afr J Bot 151:512–528. https://doi.org/10.1016/J.SAJB.2022.05.028

Benzie IFF, Strain JJ (1996) The ferric reducing ability of plasma (FRAP) as a measure of "Antioxidant Power": the FRAP assay. Anal Biochem 239:70–76. https://doi.org/10.1006/ABIO.1996.0292

Bessada SMF, Barreira JCM, Oliveira MBPP (2015) Asteraceae species with most prominent bioactivity and their potential applications: A review. Ind Crops Prod 76:604–615. https://doi.org/10.1016/J.INDCROP.2015.07.073

Bessada SMF, Barreira JCM, Barros L et al (2016) Phenolic profile and antioxidant activity of *Coleostephus myconis* (L.) Rchb.f.: An underexploited and highly disseminated species. Ind Crops Prod 89:45–51. https://doi.org/10.1016/J.INDCROP.2016.04.065

Calabrese EJ (2014) Hormesis: a fundamental concept in biology. Microb Cell 1:145–149. https://doi.org/10.15698/mic2014.05.145

Chen M, He X, Sun H et al (2022) Phytochemical analysis, UPLC-ESI-Orbitrap-MS analysis, biological activity, and toxicity of extracts from Tripleurospermum limosum (Maxim) Pobed. Arab J Chem 15:103797. https://doi.org/10.1016/J.ARABJC.2022.103797

Ćirić A, Kruljević I, Stojković D et al (2019a) Comparative investigation on edible mushrooms Macrolepiota mastoidea, *M. rhacodes* and *M. procera*: Functional foods with diverse biological activities. Food Funct. https://doi.org/10.1039/c9fo01900f

Ćirić AD, Petrović JD, Glamočlija JM et al (2019b) Natural products as biofilm formation antagonists and regulators of quorum sensing functions: a comprehensive review update and future trends. S Afr J Bot 120:65–80. https://doi.org/10.1016/j.sajb.2018.09.010

Crozier A, Del Rio D, Clifford MN (2010) Bioavailability of dietary flavonoids and phenolic compounds. Mol Aspects Med 31:446–467. https://doi.org/10.1016/J.MAM.2010.09.007

Dănilă AI, Ghenciu LA, Stoicescu ER et al (2024) Aldose reductase as a key target in the prevention and treatment of diabetic retinopathy: a comprehensive review. Biomedicines 12:747. https://doi.org/10.3390/BIOMEDICINES12040747

Guru A, Lite C, Freddy AJ et al (2021) Intracellular ROS scavenging and antioxidant regulation of WL15 from cysteine and glycine-rich protein 2 demonstrated in zebrafish *in vivo* model. Dev Comp Immunol 114:103863. https://doi.org/10.1016/J.DCI.2020.103863

Haddad M, Cherchi F, Alsalem M et al (2023) Adenosine receptors as potential therapeutic analgesic targets. Int J Mol Sci. https://doi.org/10.3390/IJMS241713160

Haridevamuthu B, Ranjan Nayak SPR, Murugan R et al (2024) Prophylactic effects of apigenin against hyperglycemia-associated amnesia via activation of the Nrf2/ARE pathway in zebrafish. Eur J Pharmacol 976:176680. https://doi.org/10.1016/J.EJPHAR.2024.176680

Hopkins AL (2008) Network pharmacology: the next paradigm in drug discovery. Nat Chem Biol 4:682–690. https://doi.org/10.1038/nchembio.118

Issac PK, Guru A, Velayutham M et al (2021) Oxidative stress induced antioxidant and neurotoxicity demonstrated in vivo zebrafish embryo or larval model and their normalization due to morin showing therapeutic implications. Life Sci 283:119864. https://doi.org/10.1016/J.LFS.2021.119864

Ivanov M, Gašić U, Stojković D et al (2021) New Evidence for *Artemisia absinthium* L. application in gastrointestinal ailments: ethnopharmacology, antimicrobial capacity, cytotoxicity, and phenolic profile. Evidence-Based Compl Alt Med. https://doi.org/10.1155/2021/9961089

Ivanov M, Ćirić A, Stojković D (2022) Emerging antifungal targets and strategies. Int J Mol Sci. https://doi.org/10.3390/IJMS23052756

Kibble M, Saarinen N, Tang J et al (2015) Network pharmacology applications to map the unexplored target space and therapeutic potential of natural products. Nat Prod Rep 32:1249–1266. https://doi.org/10.1039/C5NP00005J

Lamponi S, Aguiar C, Costa D et al (2023) The genus *Tripleurospermum* Sch. Bip. (Asteraceae): a comprehensive review of its ethnobotanical utilizations, pharmacology, phytochemistry, and toxicity. Life 13:1323. https://doi.org/10.3390/LIFE13061323

Li S, Zhang B (2013) Traditional Chinese medicine network pharmacology: theory, methodology and application. Chin J Nat Med 11:110–120. https://doi.org/10.1016/S1875-5364(13)60037-0

Lien CF, Chen SJ, Tsai MC, Lin CS (2021) Potential role of protein kinase c in the pathophysiology of diabetes-associated atherosclerosis. Front Pharmacol. https://doi.org/10.3389/FPHAR.2021.716332

Muthulakshmi L, Suganya K, Murugan M et al (2022) Antibiofilm efficacy of novel biogenic silver nanoparticles from *Terminalia catappa* against food-borne *Listeria monocytogenes* ATCC 15313 and mechanisms investigation in vivo and in vitro. J King Saud Univ Sci 34(5):102083. https://doi.org/10.1016/j.jksus.2022.102083

Najmi A, Javed SA, Al Bratty M, Alhazmi HA (2022) Modern approaches in the discovery and development of plant-based natural products and their analogues as potential therapeutic agents. Molecules. https://doi.org/10.3390/MOLECULES27020349

Nehru S, Guru A, Pachaiappan R et al (2024) Co-encapsulation and release of apigenin and ascorbic acid in polyelectrolyte multilayer capsules for targeted polycystic ovary syndrome. Int J Pharm 651:123749. https://doi.org/10.1016/J.IJPHARM.2023.123749

Nitti M, Marengo B, Furfaro AL, Pronzato MA, Marinari UM, Domenicotti C, Traverso N (2022) Hormesis and oxidative distress: pathophysiology of reactive oxygen species and the open question of antioxidant modulation and supplementation. Antioxidants (Basel) 11:1613. https://doi.org/10.3390/antiox11081613

Re R, Pellegrini N, Proteggente A et al (1999) Antioxidant activity applying an improved ABTS radical cation decolorization assay.

Free Radic Biol Med 26:1231–1237. https://doi.org/10.1016/S0891-5849(98)00315-3

Segheto L, Santos BCS, Werneck AFL et al (2018) Antioxidant extracts of coffee leaves and its active ingredient 5-caffeoylquinic acid reduce chemically-induced inflammation in mice. Ind Crops Prod 126:48–57. https://doi.org/10.1016/J.INDCROP.2018.09.027

Shaik MR, Kandaswamy K, Guru A et al (2024) Piperine-coated zinc oxide nanoparticles target biofilms and induce oral cancer apoptosis via BCl-2/BAX/P53 pathway. BMC Oral Health 24(1):715. https://doi.org/10.1186/s12903-024-04399-z

Šibul F, Orčić D, Berežni S et al (2019) HPLC–MS/MS profiling of wild-growing scentless chamomile. Acta Chromatogr 32:86–94. https://doi.org/10.1556/1326.2019.00546

Smiljkovic M, Stanisavljevic D, Stojkovic D et al (2017) Apigenin-7-O-glucoside versus apigenin: insight into the modes of anticandidal and cytotoxic actions. EXCLI J. https://doi.org/10.17179/excli2017-300

Šuk J, Mikulka J, Sen MK et al (2023) First cases of herbicide resistance of *Tripleurospermum inodorum* in the Czech Republic. Plant Soil Environ 69:81–87. https://doi.org/10.17221/427/2022-PSE

Suleimen Y, Van Hecke K, Ibatayev ZA et al (2018) Crystal structure and biological activity of matricaria ester isolated from *Tripleurospermum Inodorum* (L.) Sch. Bip J Struct Chem 59:988–991. https://doi.org/10.1134/S0022476618040352/METRICS

Sumaria N, Roediger B, Ng LG et al (2011) Cutaneous immunosurveillance by self-renewing dermal γδ T cells. J Exp Med 208:505–518. https://doi.org/10.1084/jem.20101824

Sun K, Song X, Jia R, Yin Z, Zou Y, Li L, Yin L, He C, Liang X, Yue G, Cui Q (2018) Evaluation of analgesic and anti-inflammatory activities of water extract of *Galla chinensis in vivo* models. Evid Based Complement Altern Med 2018:6784032. https://doi.org/10.1155/2018/6784032

Tammali R, Srivastava SK, Ramana KV (2011) Targeting aldose reductase for the treatment of cancer. Curr Cancer Drug Targets 11:560. https://doi.org/10.2174/156800911795655958

Tofighi Z, Molazem M, Doostdar B et al (2015) Antimicrobial activities of three medicinal plants and investigation of flavonoids of *Tripleurospermum disciforme*. Iran J Pharm Res 14:225

Tucovic D, Kulas J, Mirkov I et al (2022) Oral cadmium intake enhances contact allergen-induced skin reaction in rats. Biomed Environ Sci 35:1038–1050. https://doi.org/10.3967/bes2022.132

Victor K, Boris L, Athina G et al (2018) Design, synthesis and antimicrobial activity of usnic acid derivatives. MedChemComm 9(5):870–882. https://doi.org/10.1039/c8md00076

Zeljković SĆ, Ayaz FA, Inceer H et al (2015) Evaluation of chemical profile and antioxidant activity of *Tripleurospermum insularum*, a new species from Turkey. Nat Prod Res 29:293–296. https://doi.org/10.1080/14786419.2014.968156

Zia K, Ashraf S, Jabeen A et al (2020) Identification of potential TNF-α inhibitors: from in silico to in vitro studies. Sci Rep 10:1–9. https://doi.org/10.1038/s41598-020-77750-3